Operability analysis of monopile lowering operation using different numerical approaches

Lin Li[1,2,3], Zhen Gao[1,2,3], Torgeir Moan[1,2,3]

1 Centre for Ships and Ocean Structures (CeSOS), Norwegian University of Science and Technology, Trondheim, Norway
2 Centre for Autonomous Marine Operations and Systems (AMOS), Norwegian University of Science and Technology, Trondheim, Norway
3 Department of Marine Technology, Norwegian University of Science and Technology, Trondheim, Norway

Offshore installation operations require careful planning in the design phase to minimize associated risks. This study addresses numerical modelling and time-domain simulations of the lowering operation during installation of a monopile (MP) for offshore wind turbine (OWT) using a heavy lift vessel (HLV). The purpose is to apply different numerical approaches to obtain the allowable sea states and to assess the operability. Four critical factors regarding the numerical modelling approaches for the coupled HLV-MP lowering process are studied. Those factors include wave short crestedness, shielding effects from the HLV, radiation damping from MP and the nonstationarity of the process. The influence of each factor on the allowable sea states and the operability are assessed. A large number of time-domain simulations are performed considering random waves to derive the allowable sea states. The results indicate that the radiation damping from the MP is secondary while it is essential to consider the other features. The study can be used as a reference for numerical modelling of relevant offshore operations.

KEY WORDS: MP installation, allowable sea states, heavy lift vessel, wave spreading, shielding effects, nonstationary process

INTRODUCTION

Installation of OWT components is more challenging than of land-based wind turbines. It was estimated by Moné et al. (2015) that the installation and assembly of offshore wind turbines make up 20% of the capital costs compared with around 6% for land-based wind turbines. Because of the low profit margin of the offshore wind industry, it is essential to reduce the installation costs by improving the methodology during design and planning phase.

Because of the structural simplicity and low manufacturing expenses, monopiles (MPs) are the most preferable bottom-fixed foundations for offshore wind turbines in shallow water (Thomsen, 2011; EWEA, 2014). The installation of MP consists of several steps. After arriving the offshore site, the MPs are upended to a vertical position, the then lowered through the wave zone so that it is standing vertically on the seabed. A hydraulic hammer is used to drive it into the seabed to a predetermined depth. Although MPs are easy to install compared to other more complicated structures, the installations have been carried out with various success because the challenges have not been taken seriously enough (Thomsen, 2011). Therefore, it is of great importance to evaluate and improve the allowable sea states by considering each activity during the operation. More importantly, the allowable sea states for a single operation would affect the installation efficiency of the entire wind farm. For this reason, accurate numerical models are required.

Very few studies on the installation of MPs have been published. Sarkar and Gudmestad (2013) suggested a method to install MPs by isolating the installation operations from the motion of the floating vessel using a pre-installed submerged support structure. The responses of a coupled vessel-MP system during the lowering process of the MP were studied by Li et al. (2013), where sensitivity studies regarding the mechanical couplings and the vessel type were performed and the corresponding responses were analyzed. Furthermore, they introduced a method to account for the shielding effects from the floating installation vessel during the entire lowering operation of the MP (Li et al., 2014). It was concluded that the shielding effects can greatly reduce the responses in short waves. The approach was further studied and extended to compare the performance of two lifting systems i.e., the lifting of a monopile and a jacket wind turbine foundation (Li et al., 2015a). Recommendations regarding the heading angles of the vessel during the lifting operations of the two OWT substructures were given. Moreover, the importance of radiation damping of the MP during the nonstationary lowering operation were examined by Li et al. (2015c). A new approach was proposed to implement the radiation damping effects into the time-domain simulation of the nonstationary lowering process. The study proved the importance of the radiation damping on the large diameter MPs and should be considered to avoid over-conservative results.

The previous work aimed at developing more accurate numerical methods to simulate the lifting operation of the MP, with special focus

on the nonstationary process. In those studies, some simplifications were made in the numerical model, e.g., the hydrodynamic forces on the vessel were simplified by only considering the first order wave excitation forces in Li et al. (2013, 2014, 2015c), and the hydrodynamic interaction between the floating installation vessel and the MP was not included when studying the influences of MP radiation damping in Li et al. (2015c). Wave short crestedness is another factor of influence for lifting operations (DNV, 2014) which has not been taken into consideration in the mentioned references. Moreover, the previous study did not provide the allowable sea states based on their numerical approaches. The allowable sea states are essential for planning the operations.

In addition, some simplified approaches are often applied during numerical analysis of lifting operations, e.g., excluding the hydrodynamic interaction between submerged structures, and using steady-state analysis to represent nonstationary or transient operation activities. Those simplifications introduce uncertainties. However, the influences of the simplifications on the allowable sea states and the operability have not been quantified. Over-conservative results may increase the costs of the operation while non-conservative results may increase the operational risk.

This paper is an extension of the previous work on MP lowering operation focusing on numerical studies. The purpose is to use different numerical approaches to evaluate the allowable sea states and quantify their influences on the operability. The numerical approaches in this paper deal with the following issues: 1) the accuracy to use Morison's formula to calculate the hydrodynamic forces on the MP; 2) the effect from hydrodynamic interaction between the installation vessel and the MP on the lowering operation; 3) the feasibility to use simplified steady-state simulations for the nonstationary lowering process; 4) the influence of short crestedness for such operation.

First, a general description of the operation and the numerical model is given. Second, the dynamic modelling approach including different numerical approaches are presented. Third, the operational criteria for the MP lowering operation is provided followed by discussion of the results. Finally, conclusions and recommendations regarding practical implementation are given.

MODELLING OF THE LOWERING SYSTEM

System Components

The system for MP lowering operation consists of a floating heavy lift vessel (HLV) and the MP substructure and they are coupled through the crane lift wire. A gripper device is placed on the deck of the vessel to avoid extreme motions of the MP during the operation. The gripper is normally composed of several hydraulic cylinders, and the details refer to Li et al. (2015d).

During the lowering operation, there is an initial gap between the hydraulic cylinder and the wall of the MP. The initial gap is chosen based on the stroke length of the hydraulic cylinders as well as the motions of the MP during lowering operation to avoid large contact forces that could cause structural damage on the hydraulic cylinders. The system set-up for the MP lowering process is illustrated in Fig. 1. The main particulars of the system components are shown in Table 1. After the MP being lowered down to the seabed and the horizontal motion of the MP is reduced compared to the lowering phase, the gripper is then closed and the hydraulic cylinders provide compression to the MP before the hammering operation starts.

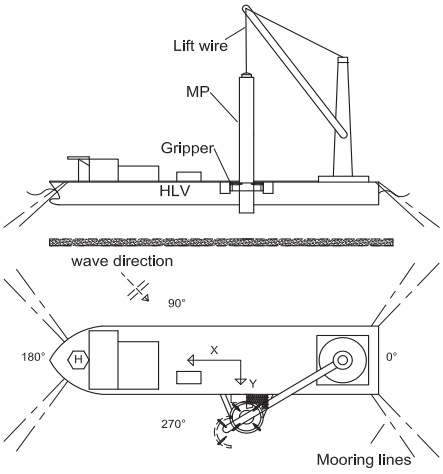

Figure 1: System set-up for the MP lowering operation using a HLV

Table 1: Structures' main particulars (Li et al., 2015d)

Parameter	Notation	Value	Units
-HLV			
Displacement		5.12E+04	Ton
Length	L	183	m
Breadth	B	47	m
Draught	T	10.2	m
Vertical position of COG above keel	VCG	17.45	m
-Monopile			
Mass	MMP	500	Ton
Diameter	DMP	5.7	m
Thickness	tMP	0.06	m
Length	LMP	60	m

Modelling of the Mechanical Couplings

The coupling between the HLV crane and the MP is achieved using a lift wire. The wire coupling force is modelled as a linear spring force, and the crane flexibility is accounted for. A winch is modelled for the crane which increases the lift wire length to lower the MP towards the sea bed.

The gripper device was modelled as a contact point attached to the vessel by Li et al. (2014). During the lowering of the monopile, the model was able to calculate the contact force between the HLV and the MP with changing position of the MP. During the lowering operation, the hydraulic cylinder rods are normally retracted and the gap between the hydraulic cylinder and the MP allows certain relative motions between the MP and the gripper. On the other hand, the relative motion of the MP and the gripper will cause large axial loads and damage in the hydraulic cylinders if the gaps between the hydraulic cylinders and the MP are too small. When the initial gap between the cylinder and the MP was chosen around 10 cm, it was found by Li et al. (2014) huge impact force occurred. In the present numerical model, the gripper device is excluded, but the relative motions between the MP and the HLV are calculated. The relative motions should be kept within a limit to avoid large impact force to ensure the structural integrity of the hydraulic cylinders.

Equations of Motion for Coupled Dynamic Analysis

The HLV-MP coupled dynamic system has 12 degrees of freedom (DOF s), and for each body, the following six equations of motion are solved in the time-domain (MARINTEK, 2012).

$$\left(\mathbf{M}+\mathbf{A}(\infty)\right)\cdot\ddot{\mathbf{x}}+\mathbf{D}_1\dot{\mathbf{x}}+\mathbf{D}_2 f(\dot{\mathbf{x}})+\mathbf{K}\mathbf{x}+\int_0^t \mathbf{h}(t-\tau)\dot{\mathbf{x}}(\tau)d\tau = \mathbf{F}_{ext}(t)=\mathbf{q}^{(1)}{}_{WA}+\mathbf{q}^{(2)}{}_{WA}+\mathbf{F}_{moor}+\mathbf{F}_{cpl} \quad (1)$$

where, $\mathbf{M}$ is the total mass matrix; $\mathbf{x}$ is the rigid-body motion vector; $\mathbf{A}(\infty)$ is the frequency-dependent added mass matrix at infinite wave frequency; $\mathbf{D}_1$ and $\mathbf{D}_2$ are the linear and quadratic damping matrices; The viscous effects from the vessel hull and the mooring system were simplified into linear damping terms in surge, sway and yaw. The roll damping of the vessel as well as the quadratic damping on the MP were also included. Additionally, $\mathbf{K}$ is the coupled hydrostatic stiffness matrix from the HLV and the MP; $\mathbf{h}$ is the retardation function calculated from the frequency-dependent added mass or potential damping and $\mathbf{F}_{ext}(t)$ is the external force vector that includes the first and second order wave excitation forces $\mathbf{q}^{(1)}{}_{WA}$ and $\mathbf{q}^{(2)}{}_{WA}$, the mooring line forces for the HLV $\mathbf{F}_{moor}$ and the coupling forces between the HLV and MP $\mathbf{F}_{cpl}$. The second-order wave excitation forces on the HLV were obtained based on the Newman's approximation and only included the difference-frequency slowly varying forces (Newman, 1974). The eight catenary mooring lines for the HLV were also modelled, and both quasi static analysis and a simplified dynamic analysis accounting for the effect of drag loading on the lines were applied.

Different approaches for the hydrodynamic modelling on the MP are explained in Sec. 3.

Natural Frequencies of the Coupled System

The natural modes of the coupled HLV-MP system include 12 degrees of freedom (DOFs). A detailed explanation of the modes and corresponding natural periods refer to Li et al. (2015c). The gripper is excluded when calculating the natural periods because the gap between the MP and the gripper allows relative motions. Fig. 2 shows how the natural periods of the system excluding the yaw mode of MP vary with the vertical position of the MP lower tip. It should be noted that all the modes are coupled, and only the dominating DOFs are mentioned here. It is expected that in short waves the MP rotational modes (modes 02 and 03) could be excited, and in longer waves the vessel motions in the vertical plane are critical.

DIFFERENT NUMERICAL APPROACHES FOR DYNAMIC ANALYSIS

In this section, different numerical approaches are explained in detail, including the modelling of the nonstationary process, hydrodynamic forces on the MP as well as the wave spreading. Discussion of the approaches and the commonly used assumptions during numerical modelling is also presented.

Steady-state and Nonstationary Analysis Approaches

During lowering operations with structures lowered through the wave zone and towards the seabed, the dynamic features of the system change continuously. There are generally two approaches to simulate the nonstationary process (Sandvik, 2012). (1) Perform steady-state simulations in irregular waves at the most critical vertical position of the object. (2) Simulate a repeated nonstationary lowering process with different irregular wave realizations, and study the extreme response observed in each simulation. It was demonstrated that the second method provides more realistic results because an unrealistic build-up of the oscillations occurs in the stationary case (Sandvik, 2012). In principle, to provide more accurate estimates of the operations, analyses of the entire lowering process are required.

However, in order to obtain reliable statistics of the extreme responses from the nonstationary analysis, a large number of simulations is required. Furthermore, the frequency-dependence of the hydrodynamic properties based on the steady-state conditions vary with time and can not be directly applied in a nonstationary analysis. For the coupled HLV-MP model, it is challenging to include the time-varying hydrodynamic interaction between the two structures during the lowering process. Because of these issues, the simplified steady-state method is widely applied to replace the nonstationary analysis. Thus, it is useful to compare the two approaches and their influence on the allowable sea states.

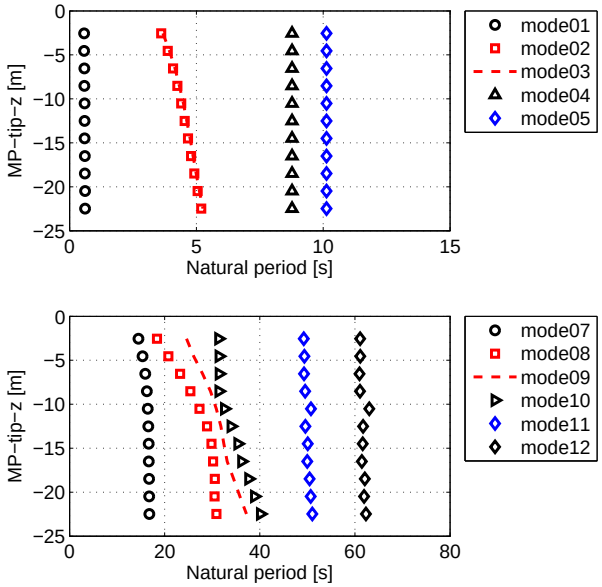

Figure 2: Natural periods for the coupled HLV-MP system with varying MP positions. Dominant motion for each mode: mode01 (MP heave); mode02 and 03 (MP roll and pitch, MP rotational motions); mode04 (HLV pitch); mode05 (HLV heave); mode07 (HLV roll); mode08 and 09 (MP pendulum motions); mode10-12 (HLV yaw, sway and surge)

Modelling of Hydrodynamic Forces on the MP

Morison's formula approximation for slender structure in incident waves

For slender bodies with a *D/L* ratio (diameter/wavelength) less than 0.20, the empirical Morison's formula is often used to calculate hydrodynamic forces (Morison et al., 1950). The effects of diffraction and radiation are considered insignificant in the slender-body approximation. The MP is divided into strips, and the wave forces $f_{W,s}$ per unit length on each strip normal to the member can be determined from Morison's formula (Faltinsen, 1990):

$$f_{W,s} = \rho_w C_M \frac{\pi D^2}{4} \cdot \ddot{\zeta}_s - \rho_w C_A \frac{\pi D^2}{4} \cdot \ddot{x}_s + \frac{1}{2} \rho_w C_q D \cdot |\dot{\zeta}_s - \dot{x}_s| \cdot (\dot{\zeta}_s - \dot{x}_s) \quad (2)$$

where, $\ddot{\zeta}_s$ and $\dot{\zeta}_s$ are fluid particle acceleration and velocity at the center of the strip, respectively; $\ddot{x}_s$ and $\dot{x}_s$ are the acceleration and velocity at the center of the strip due to the body motions; D is the outer diameter of the member; and C_M, C_A and C_q are the mass, added mass and quadratic drag force coefficients, respectively. The distributed wave forces $f_{W,s}$ are integrated along the MP to obtain the total wave forces and moments, F_W. The added mass coefficients for different strips along the MP are chosen according to Li et al. (2015c), where the excitation forces calculated using Morison's formula at different drafts were compared with those from panel method and good agreement was achieved.

In addition, the nonlinear effects due to the instantaneous free surface and the instantaneous body positions can be also included in the time-domain by evaluating at each time step and in each strip for instantaneous body positions and integrating up to the instantaneous free surface. The Morison's formula can be applied for both steady-state analysis and nonstationary lowering analysis. Both incident wave kinematic and the disturbed waves that include the shielding effects from the HLV can be used in the formula.

Multi-body hydrodynamics using potential theory

The hydrodynamic interaction between the HLV and the MP changes their individual hydrodynamic properties, including wave excitation forces, potential added mass and damping coefficients. The interaction should be properly included if the two structures are in close vicinity, e.g., the hydrodynamic interaction between a transport barge and a floating crane vessel during lift-off operations (Mukerji, 1988; van den Boom et al., 1990; Baar et al., 1992). These studies showed that the hydrodynamic interaction had little effect on the responses of the crane tip, but affected the responses of the transport barge because of the small dimension of the barge compared with the crane vessel (Baar et al., 1992). In this case, the hydrodynamic interaction is expected to affect the responses of the MP greatly.

According to the linear wave potential theory, the total velocity potential is expressed by (Lee, 1995):

$$\varphi = \varphi_D + \varphi_R = \varphi_I + \varphi_S + \varphi_R \quad (3)$$

where φ_D is the diffraction potential and φ_R is the radiation potential. φ_D can be further broken down into the sum of the incident velocity potential φ_I and the scattering velocity potential φ_S, which represents the disturbance to the incident wave caused by the presence of the body. The radiation potential itself is a linear combination of the components corresponding to the modes of motion such that

$$\varphi_R = i\omega \sum_{k=1}^{6} \xi_k \varphi_k \quad (4)$$

Here ξ_k is the complex amplitude of the oscillatory motion in mode k of the six degrees of freedom, and φ_k is the corresponding unit-amplitude radiation potential. For multi-body case, the boundary condition for the diffraction problem has changed by adding additional body surfaces. The decomposition of the radiation potential into components, corresponding to the modes of the rigid body motion, can be extended to multi-body interaction. This is done by defining φ_k as the velocity potential corresponding to a particular mode of one body while the other bodies are kept stationary. In this way, the total radiation potential consists of $6N$ components, where I is the number of bodies.

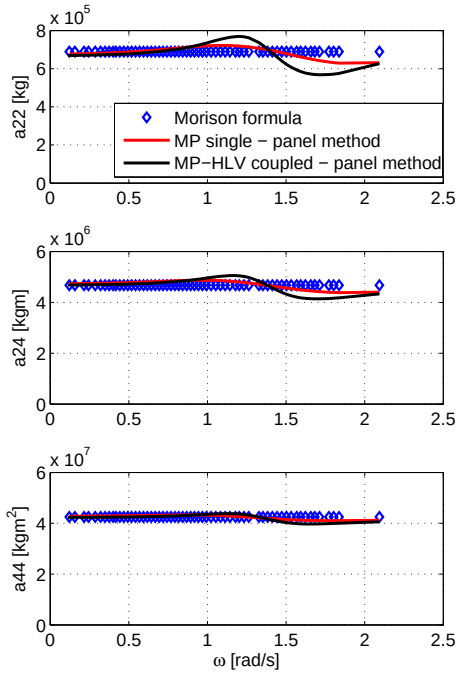

(a) added mass

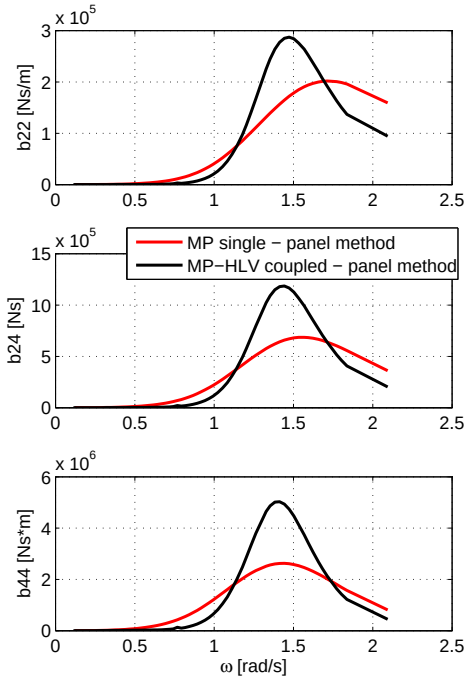

(b) damping

Figure 3: Comparison of added mass and damping of MP alone and when coupled with HLV using panel method(draft = 15 *m*)

By applying boundary conditions, the boundary value problem can be solved by numerical methods such as the panel method in the frequency domain. In this study, the panel method program WADAM is applied (DNV, 2008). The results show the HLV affects the

properties of the MP in sway and roll more significantly compared to in surge and pitch due to the small distance in *Y* direction between the two structures. Fig. 3 compares the added mass and damping of MP alone and when it is coupled with HLV. The fluctuation of added mass with wave frequency increases when the MP is placed close to the HLV. A great increase of damping in the short wave range (around 1.5 *rad*/*sec*) is visible. Those changes come from the scattered waves generated from HLV when the MP oscillates around its mean position. The effect of hydrodynamic interaction on the excitation force on the MP will be shown later in this section.

Simplified approach to consider shielding effects using Morison's formula for nonstationary process

In the current study, the hydrodynamic effects of the MP on the HLV are minor and can be neglected. However, the wave field near the HLV is altered from the original incident waves, and three-dimensional effects occur due to the diffraction and radiation from the vessel. Thus, the hydrodynamic interaction between HLV and MP can be simplified as "one-way" interaction by considering the shielding effects from the HLV on the MP while ignoring the effects from the MP on the HLV. Moreover, the multi-body hydrodynamic properties using potential theory are based on a steady-state condition with a fixed mean draft of all structures and can not be directly applied for the nonstationary analysis. Therefore, the approach proposed by Li et al. (2014) is applied to calculate the forces on MP.

This method is based on the slender body assumption, so that the wave field is assumed to be only affected by the HLV. The boundary value problem for the single body HLV in the wave field is solved bypotential theory. Thus, the hydrodynamic coefficients of the vessel and the fluid kinematics at any point in the wave field in the frequency domain can be acquired. The waves affected by both radiation and diffraction of the vessel are defined as disturbed waves, which includes the vessel shielding effects, and the undisturbed waves are defined as incident waves. The following steps are followed to calculate the forces on the MP for the nonstationary process.

1) First, generate time series of disturbed fluid kinematics at pre-defined wave points near the MP using the fluid kinematics transfer functions from potential theory considering the radiation and diffraction of the HLV.

2) Then, perform time-domain simulations. At each time step, find the closest pre-defined wave points for each strip on the MP. By applying a 3D linear interpolation between those wave points, the kinematics (elevations, fluid velocities and accelerations) at the center of each strip in disturbed waves are acquired.

3) Calculate the forces at each strip using the disturbed wave kinematics by Eq. (2) and integrate along the submerged part of the MP to get the total wave forces. Note that the draft of the MP changes continuously during the nonstationary process. The total wave forces on the MP are then used to obtain the motions of the coupled HLV-MP system. The details of this approach can be found in Li et al. (2014).

To validate whether the slender structure assumption is reasonable to calculate MP wave forces, Fig. 4 compares the wave excitation force on the MP at a draft of 15 m for four cases: (1) MP alone using panel Method; (2) MP alone using Morison's formula in incident wave; (3) HLV-MP coupled using panel method and (4) HLV-MP coupled using Morison's formula.

It is evident that the shielding effects from the HLV (coupled HLV-MP case) reduce the excitation force on MP significantly in intermediate to short wave length. Good agreement between the Morison's formula and the panel method is observed with wave frequency less than 1.5 *rad*/*sec* in incident waves. For the HLV-MP coupled case, i.e., the disturbed wave case, the slender structure assumption is suitable even for shorter wave conditions because of the great reduction from the shielding effects due to HLV. In addition, the added mass calculated from 2D coefficients used in Morison's formula are compared with the one from panel method, see Fig. 3 (a). The results show good agreement between the slender structure assumption and the multi-body potential theory in terms of hydrodynamic properties. Therefore, the simplified shielding effects approach is considered reasonable to calculate wave excitation force on the MP for the HLV-MP coupled condition during the nonstationary lowering process.

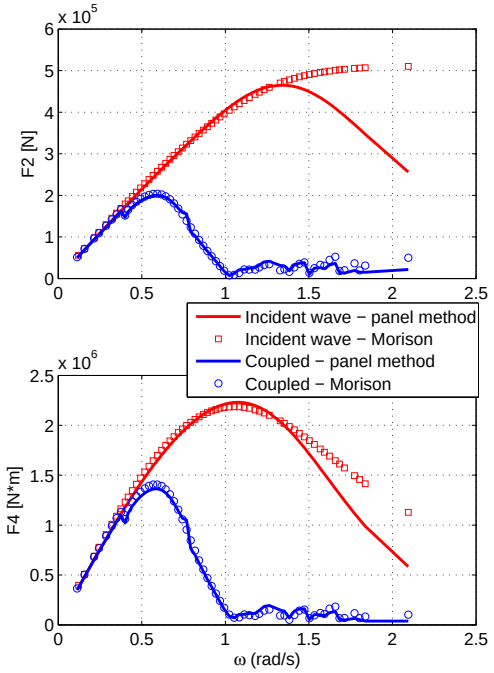

Figure 4: Comparison of excitation force on MP in incident wave and when accounting for shielding effects due to the HLV (*Dir* = 90 *deg*, draft = 15 *m*)

Morison's formula plus radiation damping for nonstationary process

As discussed previously, Morison's formula does not account for the radiation and diffraction of the structure, and the coefficients from potential theory cannot be directly applied in the nonstationary case with time-varying draft of the structure. Li et al. (2015c) concluded that the radiation damping on the large diameter MP is of importance especially for short wave conditions in incident waves. However, the hydrodynamic interaction between the HLV and the MP was not included in Li et al. (2015c), and the influences of the radiation damping of the MP in short waves for the coupled case were unknown. This study compares the effects by implementing the radiation damping on the MP for the coupled HLV-MP case.

The approach proposed by Li et al. (2015c) is applied to implement the radiation damping effects of the nonstationary process by interpolating the retardation functions at pre-defined drafts of the MP in the time-domain. The hydrodynamic interaction between the HLV

and the MP is accounted for when implementing the retardation functions for MP for the current model. The radiation damping of the MP is included together with the shielding effects from the HLV to include the complete hydrodynamic interaction. Fig. 3 shows the added mass and damping of the MP without and with the HLV. The retardation function is computed using a transform of the frequency-dependent added mass and damping from the coupled HLV-MP case to be used in the time-domain simulations.

Short-crested Waves and Shielding Effects

A wave condition is classified as long-crested and short-crested based on the directions of wave propagation. Wind generated seas in real sea conditions involve short-crested waves (Chakrabarti, 1987; Goda, 2010; Kumar et al., 1999). The directional spreading of wave energy may give rise to forces and motions which are different from those corresponding to long-crested waves.

DNV (2014) recommends to check "whether long crested or short crested sea is conservative for the analysis concerned". For head sea short crested sea will give increased roll motion of the crane vessel compared to long crested sea, while long crested sea will give increased pitch motion compared to short crested sea. It is therefore necessary to carry out analysis to conclude on this aspect. This study evaluates the influence of the short crestedness when including the shielding effects from the HLV on the responses of the MP lowering system.

The sea state is often represented by a wave spectrum as (DNV, 2014)

$$S(\omega,\theta) = S(\omega)D(\omega,\theta) \tag{5}$$

$$\int_{-\pi}^{\pi} D(\omega,\theta)d\theta = 1 \tag{6}$$

For practical purposes, the frequency dependence of the directional function is neglected, that is, $D(\omega,\theta) = D(\theta)$. One of the most widely used $D(\theta)$ is the cosine power function given as

$$D(\theta) = \begin{cases} C(n)\cos^n(\theta-\theta_0) & |\theta-\theta_0| \le \pi/2 \\ 0 & |\theta-\theta_0| > \pi/2 \end{cases} \tag{7}$$

where θ_0 is the main wave direction about which the angular distribution is centered. The parameter n is a spreading index describing the degree of wave short crestedness, with $n\to\infty$ representing a long-crested wave field. $C(n)$ is a normalizing constant ensuring that Eq. (6) is satisfied. Typical values for the spreading index for wind generated sea are n = 2 to 4. Because lifting operations are usually carried out in relatively low sea states, the spreading of the waves could be significant.

For long-crested waves, knowing incident wave realization $x(t)$, the Fourier transform of the kinematics of the disturbed wave $Y(\omega, \theta_0)$ can be calculated in the frequency domain based on $X(\omega)$, the Fourier transform of $x(t)$, and the disturbed fluid kinematics transfer functions $H(\omega, \theta_0)$, i.e., Eq. (8).

$$Y(\omega,\theta_0) = H(\omega,\theta_0)\cdot X(\omega) \tag{8}$$

For short-crested waves, the incident wave realization includes different wave direction components and is generated from the two-dimensional wave spectrum in Eq. (5). The Fourier transform of the incident wave at various directions $X(\omega, \theta)$ can be obtained. Thus, the disturbed fluid kinematics for direction θ_0 in short-crested waves are obtained as follows.

$$Y(\omega,\theta_0) = \int_{\theta_1}^{\theta_2} H(\omega,\theta)X(\omega,\theta)d\theta \tag{9}$$

where θ_1 and θ_2 are the limits for the directions. Using Eq. (2) and the disturbed wave kinematics from Eq. (9), the excitation forces on the MP accounts for both shielding effects and short-crested waves and can be applied in the nonstationary lowering analysis.

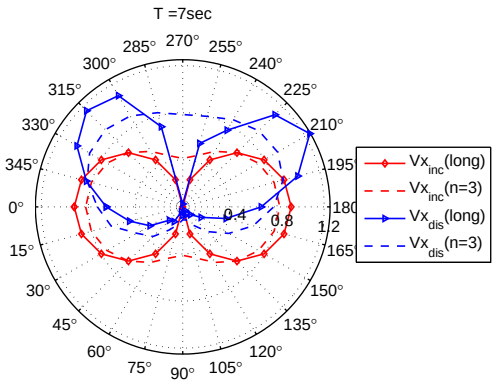

Figure 5: RAOs of fluid X-velocities in incident and disturbed waves with and without wave spreading (T = 7 *sec*)

Fig. 5 gives an example of the RAOs of fluid particle X-velocity near the MP in incident and disturbed waves considering wave spreading. The shielding effects are clearly visible in that the RAOs in disturbed waves are greatly affected by the HLV. The RAOs in the leeward side of the HLV (from 0 *deg* to 180 *deg*) are significantly reduced for given wave period in disturbed waves while in the windward side (from 180 *deg* to 360 *deg*) the RAOs are amplified.

When only long-crested waves are considered, the differences between the RAOs in incident and disturbed waves are significant. However, these differences can be reduced considerably when including the wave spreading. For example, the RAOs of X-velocity at T = 7 *sec* near 180 *deg* direction in disturbed waves are close to those in incident waves with spreading index n=3. This is because the spreading function averages the low RAOs in the leeward side and the large RAO values in the windward side of the vessel. It can be predicted that the shielding effects in short-crested waves will be less pronounced compared with the case when only long-crested waves are considered.

TIME-DOMAIN SIMULATIONS AND CASE STUDIES

Case studies are performed to study the influence of different approaches on the allowable sea states. The factors used in the case studies are summarized in Table 2. Five cases are defined for the HLV-MP lowering analysis. Among those, Case 1 accounts for all the factors that might affect the response of the system and represents the most accurate numerical method, while the other cases neglect one or two factors in order to study the influence of each factor.

The spreading index n=3 (see Eq. (7)) is used for the cases considering short-crested waves. For nonstationary lowering simulation, the winch in the crane starts from 300 *sec* to 740 *sec* with a speed of 0.05 *m*/*s*. The total lowering length was 22 *m*. Twenty repetitions of the lowering simulation are performed, corresponding to a duration of approximately two hours. The maximum relative motions between the HLV and the MP at the gripper position during the 20 simulations are used as characteristic responses to determine the allowable sea states.

The most onerous draft of the MP are found from the nonstationary lowering simulation, and 20 steady-state simulations are carried out. The same simulation length as the nonstationary simulations is applied, and the maximum relative motions are used to determine the allowable sea states for the steady-state simulation.

Step-by-step integration methods combined with an iterative routine were applied to calculate the responses of the lowering system. The equations of motion were solved by Newmark-beta numerical integration scheme with a time step of 0.02 *sec*. The first and second order wave forces of the HLV were pre-generated using Fast Fourier Transformation (*FFT*) at its mean position. The wave forces on the MP are calculated in an external Dynamic Link Library (DLL) and interacts with SIMO program (MARINTEK, 2012) where the motions of the coupled system are solved in the time-domain.

Table 2: Factors for case study in the time-domain simulations

Factors	A wave spreading	B shielding effects	C MP radiation	D Nonstationary
(1)	long-crested	incident wave	no radiation damping	steady-state simulation
(2)	short-crested	disturbed wave	radiation damping	lowering simulation
Simulation Cases		HLV-MP lowering system		
Case 1 (*A2B2C2D2*)	short-crested	disturbed wave	radiation damping	lowering simulation
Case 2 (*A1B2C2D2*)	long-crested	disturbed wave	radiation damping	lowering simulation
Case 3 (*A2B1C1D2*)	short-crested	incident wave	no radiation damping	lowering simulation
Case 4 (*A2B2C1D2*)	short-crested	disturbed wave	no radiation damping	lowering simulation
Case 5 (*A2B2C2D1*)	short-crested	disturbed wave	radiation damping	steady-state simulation

OPERATIONAL CRITERIA

The operational limits in terms of allowable sea states for installing a MP should be established by assessing all installation phases, including the upending, lowering and hammering operations. However, this study is limited to the lowering phase. The potential critical events that can limit the operation in this phase are as follows.

- Lift wire breakage. The tension in the lift wire should never exceed the maximum working load of the wire. A slack wire and snap forces should both be avoided.

- Large MP tip displacement before landing. The motions of the monopile, particularly its rotations and the displacements of its end tip, affect the landing process that follows the lowering process. Large excursion of the MP tip may result exceeding distance from the designed installation position. Moreover, the correction of the large inclination angle before hammering may exceed the capability of the hydraulic cylinders due to the limits of the stroke length.

- Failure of the hydraulic system in the gripper device. The exceedance of the allowable forces on the system will result in a hydraulic system failure. The failure will not only stop the operation but also may pollute the environment if leakage of hydraulic fluid occurs.

Because no slings are applied for the lifting arrangement, the main lift wire tension is observed to be stable and no snap loads occur. The installed position of the MP can vary from the designed position in a relatively large range (around 2 *m*), which exceeds the motions of the MP in the operational sea states. In addition, the inclination angle after landing can be adjusted by moving the HLV using mooring lines and thus not considered as critical (Li et al., 2015d).

In this study, only the failure of the hydraulic system in the gripper device is considered as a critical event for determining the operational sea states. The corresponding limiting response parameter is the allowable gap between the MP and HLV at the gripper position. Due to large stiffness of the hydraulic cylinders, impact forces occur when the relative motion exceeds the allowable gap. Based on the dimension of the MP and the most common designs for the hydraulic cylinders used in the industry, the allowable gap is chosen as 1 m. Therefore, the sea states which result in relative motions at the gripper position larger than this allowable limit are considered unacceptable. This criterion is used to decide the allowable sea states for MP lowering operation.

RSULTS AND DISCUSSIONS

From time-domain simulations at various wave conditions, the allowable sea states are obtained by applying the operational criteria. Different modelling approaches are applied for the corresponding cases. The results are presented with discussions in this section.

Effect of the Hydrodynamic Load Modelling Approach

Figure 6 compares the allowable *Hs* and *Tp* values for Cases 1, 3 and 4. Case 1 is the most accurate approach including all the features shown in Table 2, while Case 3 neglects the MP radiation damping and the shielding effects, e.g., the hydrodynamic couplings between the HLV and MP. Case 4 includes shielding effects but neglects the MP radiation damping. The maximum *Hs* values occur at wave period around 7 *sec* for Case 1. The short waves excite the MP rotational resonance motions and the long waves excite the HLV motions in the vertical plane (see the natural periods of the system in Fig. 2), and thus the *Hs* values decrease for those conditions.

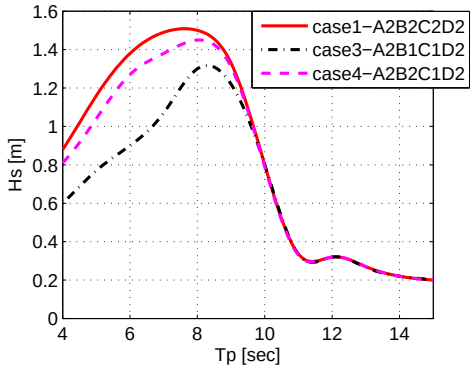

Figure 6: Comparison on allowable sea states for Cases 1, 3 and 4

Figure 7 presents the MP pitch motions in two representative sea states for the three cases. The shielding effects from the HLV are observed critical and the resonance motions of the MP ($\omega \approx 1.2$ *rad*/*s*) are overestimated greatly for Case 3 without shielding effects (see Fig. 7 (a)). The allowable sea states are thus significantly underestimated (Fig. 6 Case 3). The effects appears more significant in short waves than in long waves due to the large diffraction from the vessel in short waves. The shielding effects can be ignored for wave period larger than 10 *sec* when assessing the allowable sea states. Case 3 represents the most commonly applied simplification calculating the hydrodynamic forces on slender structures using Morison's Formula in incident waves. The results here prove a great underestimation of the allowable sea states for the MP lowering operation using this simplification.

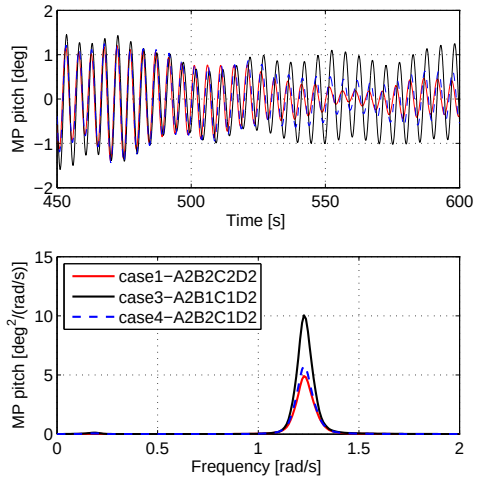

(a) *Hs* = 1.0 *m*, *Tp* = 5 *s*, *Dir* = 150 *deg*

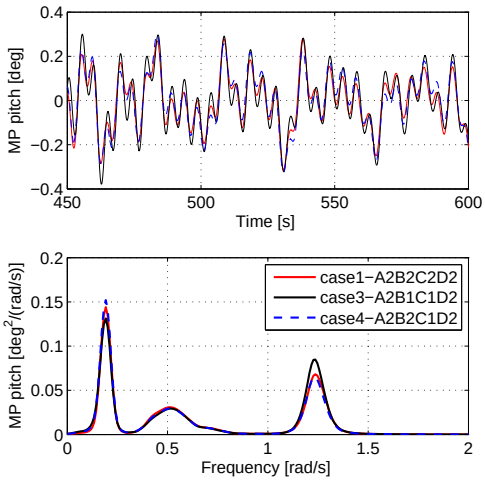

(b) *Hs* = 0.3 *m*, *Tp* = 12 *s*, *Dir* = 180 *deg*

Figure 7: Response time series and spectra of MP pitch for Cases 1, 3 and 4

The responses in Fig. 7 also show that the MP radiation damping effects are secondary compared with the shielding effects. Larger peak is observed at the MP resonance frequency in short waves, and the differences are negligible in long waves. The exclusion of the radiation damping underestimates the *Hs* values by around 0.1*m* for wave period less than 8 *sec*, and the *Hs* values are almost the same as those from Case 1 for longer waves.

Effect of Wave Spreading

Another commonly applied simplification during numerical simulation is to exclude the wave spreading by using long-crested waves. Figure 8 displays the allowable sea states by using long- and short-crested waves. For wave period less than 12 *sec*, the long-crested assumption greatly overestimates the significant wave heights. The spectra of MP roll and pitch motions at two wave conditions for Cases 1 and 2 are presented in Fig. 9. For both sea states, one can observe large differences in the spectra. In short waves, the long-crested wave assumption provides much lower responses at the resonance frequency (Fig. 9 (a)). As mentioned, the shielding effects are significant in short waves, however, the spreading of the waves averages the low wave kinematics in the leeward side of the vessel and the high values in the windward side, see Fig. 5. Thus, the MP experiences less shielding effects from the HLV for the same heading angles in short-crested waves than in long-crested waves, which results in higher allowable sea states in short waves, as shown in Fig. 8.

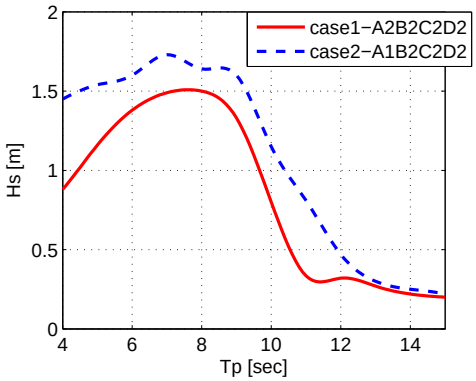

Figure 8: Comparison on allowable sea states for Cases 1 and 2

In longer waves, the shielding effects are minor. However, the spreading of the waves increases the HLV motions in the transverse direction, e.g., roll motions. Thus, MP experiences larger responses in short-crested waves in roll, see Fig. 9(b) top, where the spectra density of roll near the wave frequency for Case 1 are much higher than Case 2 with long-crested waves. The pitch motions at the resonance frequency are lower using short-crested waves in this condition due to lower wave energy presented in the longitudinal direction at heading seas. Because of the significant increase of the transverse motions in short-crested waves, and resulting allowable sea states are lower than in long-crested waves. For operational sea states with *Hs* less than 2m, the waves are normally dominated by short-crested wind seas. Thus, the spreading of the waves should be taken into consideration to avoid non-conservative allowable sea states.

Comparison between Steady-state and Nonstationary Analysis

From the nonstationary lowering simulation, the most critical MP drafts result in the largest responses are obtained for each wave peak period. It was found for most of the wave conditions, the most critical situation occurs when the MP draft is very shallow (around 2 to 3 m). With this draft, the gripper position is far from the COG of the MP and a small rotational angle of the MP gives large relative motions between the HLV and the MP. Another reason is that the MP experiences less damping at a smaller draft compared to those with increasing draft. Steady-state simulations at the most critical drafts are performed and the corresponding allowable sea states are compared with those from the nonstationary lowering simulations in Fig. 10.

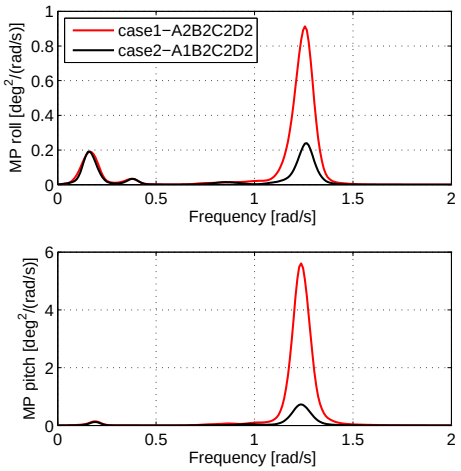

(a) *Hs* = 1.4 *m*, *Tp* = 6 *s*, *Dir* = 150 *deg*

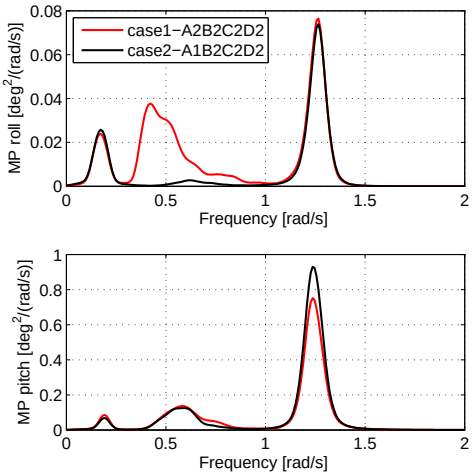

(b) *Hs* = 0.8 *m*, *Tp* = 10 *s*, *Dir* = 180 *deg*

Figure 9: Response spectra of MP rotational motions for Cases 1 and 2

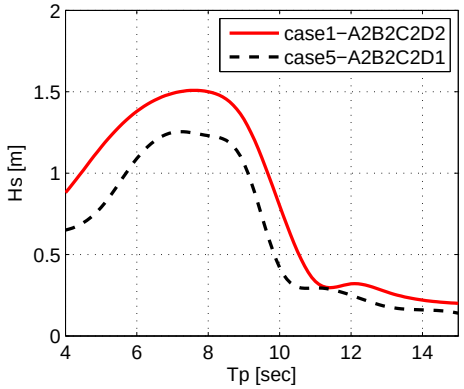

Figure 10: Comparison on allowable sea states for Cases 1 and 4

A considerable reduction of the allowable *Hs* value can be observed for almost all *Tp* conditions. The reduction appears to be more significant in shorter waves due to the resonance motions are accelerated in the steady-state analysis. Although the steady-state analysis provide conservative results, it may greatly increase the downtime and costs for the operation.

Effects of Vessel Heading Angles on the Allowable Sea States

Because the shielding effects and the vessel motions are sensitive to the wave direction, three heading angles of the HLV are applied in the time-domain simulation, i.e., 150 *deg*, 165 *deg* and 180 *deg*. Fig. 11 shows the allowable sea states for Case 1 with different heading angles, and the maximum sea states for each *Tp* values are also shown in circles. One can observe that the system prefers 150 *deg* in short waves with *Tp* less than 7 *sec*. The most proper heading moves to 165 *deg* and then to heading seas in long waves. This is because the shielding effects from the HLV are stronger for the MP close to quartering seas in short waves. In long waves, the shielding effects are minor, but the motions of the vessel increase greatly when the heading moves away from the heading seas because of the increasing transverse motions caused by short-crested waves.

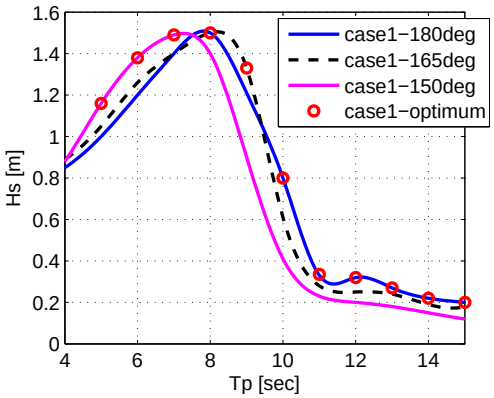

Figure 11: Comparison on allowable sea states for Case 1 with different heading angles

Figure 12 presents the most preferable heading angles which give the maximum allowable *Hs* values for three different cases. Case 1 and 2 show similar trend, but Case 3 results in different angles in short waves. This is because Case 3 excludes the shielding effects from the HLV and the most suitable headings are close to the heading seas to avoid large transverse motions of the vessel. Thus, the most preferable headings are affected by the approach applied in the numerical models.

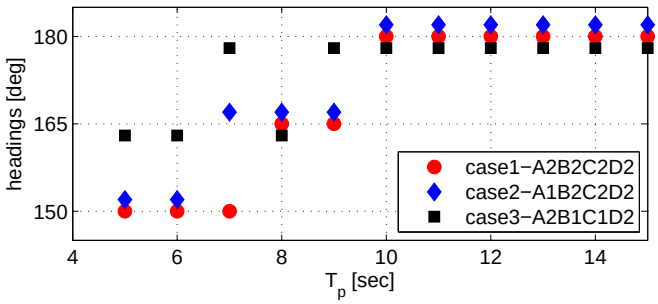

Figure 12: Comparison on the most preferable heading angles for Cases 1, 2 and 3

The allowable sea states presented in Fig. 6 and 8 correspond to the most preferable headings shown in Fig. 12. For Case 4 and Case 5, the

headings are the same as Case 1 since all three cases consider both shielding effects and short-crested waves which are the only two heading-dependent factors.

Operability analysis

For weather sensitive marine operations, it is useful to evaluate the probability of acceptable weather conditions. For this study, it is also important to show the influences of different factors affecting on the operational probability for a typical site. The wave data from the North Sea Centre site in Li et al. (2015b) was chosen for the operability analysis. This site is suitable for MP foundations with an average water depth of 29 m, and the location is close to the Dogger Bank wind farm. The wave date were hourly sampled and generated from a hindcast model from 2001 to 2010. The wave data from April to September are used for the operability study, and the corresponding 10-year scatter diagram is shown in Table 4. The operational sea states from Cases 1, 2 and 3 are highlighted in the table.

Assuming the MP lowering operation lasts for one hour, the corresponding operability for different cases are therefore calculated for this site using the derived allowable sea states. Table 3 presents the operability for different cases using the most preferable headings as well as the results from Case 1 using fixed headings. The absolute errors of the operability for different cases are also shown with respect to Case 1 which applies the most accurate numerical model.

Table 3: Operability for MP lowering at North Sea Center in the period from April to September using different methods and heading angles

Method	Operability (%)	absolute error w.r.t Case 1 (%)
Case 1 (*A2B2C2D2*)	57.5	/
Case 2 (*A1B2C2D2*)	72.8	15.3
Case 3 (*A2B1C1D2*)	28.2	-29.3
Case 4 (*A2B2C1D2*)	50.3	-7.2
Case 5 (*A2B2C2D1*)	33.4	-24.1
Case 1 (180 *deg*)	49.2	-8.3
Case 1 (165 *deg*)	52.0	-5.5
Case 1 (150 *deg*)	55.1	-2.4

Using long-crested waves overestimates the operability while the other three cases provide conservative results. The table also indicates the importance of each factor in the numerical method. For the studied scenario, the shielding effects are the most critical factor, following by the nonstationary analysis approach and the wave spreading. Although the MP radiation damping is less important than the other factors, the exclusion of the radiation damping underestimates the operability by over 7% for this site.

The comparison of the operability using three headings with the most preferable headings for Case 1 shows that it is possible to increase the operability by varying the heading of the HLV in different sea states. Because the sea states in the North Sea Center from April to September are dominated by short waves with *Tp* less than 8 *sec* (see Table 4), using 150 *deg* gives the largest operability compare with the other two headings due to the advantage of shielding effects from the HLV. However, the system may experience strong motions in longer waves with 150 *deg* heading in spreading waves.

CONCLUSITIONS AND RECOMMENDATIONS

Obtaining the allowable sea states for offshore operations in the design phase are important to minimize the risk and improve operation efficiency. The present work examines the allowable sea states and operability for the MP lowering operations using different numerical approaches.

The numerical model consists of HLV and MP with hydrodynamic interaction and mechanical couplings. The lowering process is nonstationary with time-dependent properties of the system. The factors considered in different numerical approaches include the wave spreading, the shielding effects, the MP radiation damping as well as the nonstationarity of the process. To account for the shielding effects from the HLV and the MP radiation damping during the nonstationary MP lowering process, the methods proposed by Li et al. (2014) and Li et al. (2015c) are applied. Five simulation cases are defined to study the influence of different factors. The responses obtained from time-domain simulations are evaluated with the operational criteria to acquire the allowable sea states. The main conclusions and recommendations from this study are provided as follows.

- The shielding effects from the HLV are more considerable than the radiation damping from the MP for the responses of the lowering system. Those effects are found to be critical in short waves when the diffraction of the HLV and the radiation of the MP are huge and can be neglected for waves longer than 10 *sec*.

- Long-crested wave assumption underestimate the responses and brings pronounced increase of the allowable sea states in both short and long wave conditions. The operation may experience more risks if the allowable sea states are derived using long-crested waves.

- Using steady-state analysis at a fixed draft of MP overestimates the responses compared with the nonstationary approach. The resulting allowable sea states are over-conservative in both short and long waves.

- The preferable heading angles for different sea states are obtained. The preferable heading angles change from around 150 *deg* in short waves to take advantage of the shielding effects to 180 *deg* in long waves to avoid large transverse motions of the vessel due to wave spreading.

- Operability analysis is carried out by using 10-year sea states from April to September at the North Sea Center Site. The exclusion of shielding effects, wave spreading and the nonstationarity of the process result in more than 15% absolute error in the operability analysis. The radiation damping of the MP give around 7% absolute error. It is recommend to consider the shielding effects, wave spreading in the numerical approach and use nonstationary analysis. For site conditions dominated by short waves, the radiation damping of the MP should also be included when assessing the operability.

- It is beneficial to use the most preferable headings at different sea states to increase the operability.

This study provides a basis to improve numerical analysis for nonstationary lifting operation of slender structures using a floating vessel. The considerations may be different for other types of operations. However, it is important to evaluate and quantify the influences of each factor in the numerical study to acquire reliable allowable sea states and the operability for a specific site in the design phase.

Table 4: Ten-year scatter diagram of *Hs* and *Tp* at the North Sea Center Site from April to September, with operational sea states for Cases 1, 2 and 3

Hs (*m*) \ *Tp* (*sec*)	1-2	2-3	3-4	4-5	5-6	6-7	7-8	8-9	9-10	10-11	11-12	12-13	13-14	14-15	15-16	16-17	Sum
0.1	0	0	8	0	0	3	13	0	1	6	0	0	12	0	0	0	43
0.3	3	44	461	334	74	47	80	67	46	37	27	10	6	13	10	2	1261
0.5	0	86	633	1803	788	245	152	221	165	81	28	20	31	12	4	9	4278
0.7	0	31	707	2233	1632	686	215	242	177	180	60	26	33	14	3	10	6249
0.9	0	3	228	2428	2008	1201	327	270	320	263	46	24	15	11	1	3	7148
1.1	0	0	44	1486	1816	1151	595	265	181	235	89	36	34	7	3	4	5946
1.3	0	0	3	590	1677	1017	524	278	165	194	80	36	7	13	1	0	4585
1.5	0	0	0	175	1403	878	428	233	73	91	81	45	19	4	2	0	3432
1.7	0	0	0	41	930	837	381	233	36	38	45	45	10	6	2	0	2604
1.9	0	0	0	2	472	765	324	176	66	27	15	19	38	22	4	0	1930
2.1	0	0	0	1	191	818	265	165	38	20	14	14	24	2	1	0	1553
2.3	0	0	0	0	56	569	328	140	50	9	4	10	20	1	0	0	1187
2.5	0	0	0	0	14	361	269	110	38	16	2	11	17	1	0	0	839
2.7	0	0	0	0	1	239	267	112	34	9	2	1	12	0	0	0	677
2.9	0	0	0	0	0	101	218	134	45	16	3	2	22	2	0	0	543
3.1	0	0	0	0	0	35	170	77	65	16	3	0	7	4	0	0	377
3.3	0	0	0	0	0	4	133	44	42	8	6	0	2	0	0	0	239
3.5	0	0	0	0	0	1	117	53	51	12	3	0	0	0	0	0	237
3.7	0	0	0	0	0	1	59	48	41	12	4	0	0	0	0	0	165
3.9	0	0	0	0	0	0	44	26	43	13	5	1	0	0	0	0	132
4.5	0	0	0	0	0	0	35	82	112	85	16	0	0	0	0	0	330
5.5	0	0	0	0	0	0	0	8	31	75	25	1	0	0	0	0	140
6.5	0	0	0	0	0	0	0	0	0	18	7	0	0	0	0	0	25
Sum	3	164	2084	9093	11062	8959	4944	2984	1820	1461	565	301	309	112	31	28	43920

Note: (1) Operational sea states for Case 1 are and

(2 Operational sea states for Case 2 are and and

(3) Operational sea states for Case 3 are

ACKNOWLEDGEMENTS

This work has been financially supported by the Research Council of Norway granted through the Department of Marine Technology, the Centre for Ships and Ocean Structures (CeSOS) and the Centre for Autonomous Marine Operations and Systems (AMOS), NTNU.

REFERENCES

Baar, J., Pijfers, J., Santen, J., 1992. Hydromechanically coupled motions of a crane vessel and a transport barge. In: *24th Offshore Technology Conference*, Houston.

Chakrabarti, S. K., 1987. *Hydrodynamics of offshore structures*. WIT press.

DNV, 2008. *Wadam theory manual*. Det Norske Veritas.

DNV, February 2014. *Recommended Practice DNV-RP-H103, Modelling and Analysis of Marine Operations*. Det Norske Veritas.

EWEA, 2014. *The European offshore wind industry - key trends and statistics 2013*. Report, The European Wind Energy Association.

Faltinsen, O., 1990. *Sea Loads on Ships and Ocean Structures*. Cambridge University Press. Goda, Y., 2010. Random seas and design of maritime structures. World Scientific.

Kumar, V. S., Deo, M., Anand, N., Chandramohan, P., 1999. Estimation of wave directional spreading in shallow water. *Ocean engineering* 26 (1), 83–98.

Lee, C., 1995. *WAMIT theory manual*. Massachusetts Institute of Technology, Department of Ocean

Engineering.

Li, L., Gao, Z., Moan, T., 2013. Numerical simulations for installation of offshore wind turbine monopiles using floating vessels. In: *Proceedings of the 32nd International Conference on Ocean, Offshore and Arctic Engineering*, June 9-14, Nantes, France.

Li, L., Gao, Z., Moan, T., 2015a. Comparative study of lifting operations of offshore wind turbine monopile and jacket substructures considering shielding effects. In: *The 25th International Offshore and Polar Engineering Conference*, Hawaii, USA, June 21-26.

Li, L., Gao, Z., Moan, T., 2015b. Joint distribution of environmental condition at five European offshore sites for design of combined wind and wave energy devices. *Journal of Offshore Mechanics and Arctic Engineering* 137 (3).

Li, L., Gao, Z., Moan, T., 2015c. Response analysis of a nonstationary lowering operation for an offshore wind turbine monopile substructure. *Journal of Offshore Mechanics and Arctic Engineering* 137 (4).

Li, L., Gao, Z., Moan, T., Ormberg, H., 2014. Analysis of lifting operation of a monopile for an offshore wind turbine considering vessel shielding effects. *Marine Structures* 39, 287–314.

Li, L., Guachamin Acero, W., Gao, Z., Moan, T., 2015d. Assessment of allowable sea states during installation of OWT monopiles with shallow penetration in the seabed, under review in *Journal of Offshore Mechanics and Arctic Engineering*.

MARINTEK, 2012. *SIMO - Theory Manual* Version 4.0.

Mon´e, C., Simith, A., Maples, B., Hand, M., 2015. *2013 cost of wind energy review*. Technical Report, National Renewable Energy Laboratory (NREL).

Morison, J., Johnson, J., Schaaf, S., 1950. The force exerted by surface waves on piles. *Journal of Petroleum Technology* 2 (05), 149–154.

Mukerji, P., 1988. Hydrodynamic responses of derrick vessels in waves during heavy lift operation. In: *20th Offshore Technology Conference*, Houston.

Newman, J. N., 1974. Second-order, slowly-varying forces on vessels in irregular waves. In: *International Symposium on the Dynamics of Marine Vehicles and Structures in Waves*, University College, London.

Sandvik, P., 2012. Estimation of extreme response from operations involving transients. In: *Proceedings of the 2nd Marine Operations Specialty Symposium*. Singapore.

Sarkar, A., Gudmestad, O., 2013. Study on a new method for installing a monopile and a fully integrated offshore wind turbine structure. *Marine Structures* 33, 160–187.

Thomsen, K., 2011. Offshore wind: *A comprehensive guide to successful offshore wind farm installation*. Academic Press.

van den Boom, H., Dekker, J., Dallinga, R., 1990. Computer analysis of heavy lift operations. In: *22nd Offshore Technology Conference*, Houston.